†Electronic Supporting Information (ESI)

Controllable sulphur vacancies confined in nanoporous ZnS nanoplates for visible-light photocatalytic hydrogen evolution

Jinhua Xiong[*,a,b], Yuling Li[a], Shaojuan Lv[a], Wei Guo[b], Junhua Zou[b], Zhibin Fang[*,c]

a. Fujian Provincial Key Laboratory of Clean Energy Materials, Longyan University, Longyan 364000, P. R. China.

b. State key laboratory of photocatalysis on energy and environment, Fuzhou University, Fuzhou 350002, P. R. China.

c. State Key Laboratory of Structural Chemistry, Fujian Institute of Research on the Structural of Matter, Chinese Academy of Science, Fuzhou 350002, P. R. China.

* Corresponding author: Jinhua Xiong

E-mail: xjh970996937@sina.com

* Corresponding author: Zhibin Fang

E-mail: fangzhibin@fjirsm.ac.cn

1. Experiment details

1.1 Materials

H_2PtCl_6•$6H_2O$, (A. R., Sinopharm Chemical Reagent Co. (SCRC), ethanol (EtOH, A. R., SCRC), deionized water (home-made), ethanediamine (en, A. R., SCRC), thiourea (A. R., SCRC), $ZnCl_2$ (A. R., SCRC.). N,N-dimethylformamide (DMF, A. R., SCRC), Na_2S•H_2O and Na_2SO_3 (A. R., SCRC.)

1.2 Synthsis of $ZnS(en)_{0.5}$: 0.191 g $ZnCl_2$, 0.64 g thiourea and 50 mL ethanediamine were added into 100 mL Telfon-lined autoclave and the mixture was stirred for 1 h。 Subsequently, the autoclave was sealed and maintained at 160 ^oC for 12 h and nature air cooling. The resulting white solid products were centrifuged, washed with absolute ethanol and distilled water for several times, and then dried at 40 ^oC overnight.

1.3 Synthesis of nanoporous S_v-ZnS nanoplates:

The as-prepared 40 mg $ZnS(en)_{0.5}$ was spread into a combustion boat with a capacity of 5 mL. Then, the sample was rapidly put into a muffle furnace with a temperature (T) for some time (t) and taken out immediately. T and t includes 500 ^0C and 5 min, 500 ^0C and 10 min, 460 ^0C and 10 min, 460 ^0C and 20 min, 460 ^0C and 30 min, 420 ^0C and 30 min, 350 ^0C and 30 min, respectively.

2. Characterization

2.1 X-ray diffraction (XRD) patterns were recorded on a X'Pert3 Powder X-ray diffractometer with Cu Ka radiation operated at 40 kV and 40 mA. To obtain the Transmission electron microscopy (TEM) images, high-resolution (HR) TEM images and STEM-EDX mapping, the sample was dropped on Mo grid and operated on a Talos F200S. X-ray photoelectron spectroscopy (XPS) measurements were performed on a ThermoFischer system with a monochromatic Al Kα source. XPS dates were calibrated by C_{1s}=284.8 eV. Ultraviolet-visible absorption spectra was obtained using UV-2600, $BaSO_4$ as the reference. Electron Paramagnetic resonance (EPR) signals were recorded with a Brucker A300 spectrometer. Accurate weight of 8 mg for a sample was enclosed in the EPR tube for a direct test. If irradiation was needed, simulated solar light source was used and the light was irradiated on EPR tube directly. Parameters setting was as follows: microwave power, 6.35 mW; frequency, 9.86 GHz; centre field, 3500 G; sweep width, 700 G; attenuator 15 dB; resolution, 1024 point. Field-emission scanning electron microscopy (FESEM, Carl Zeiss Sigma 300) was used to determine the morphology of the samples.

The Brunauer–Emmett–Teller (BET) surface area was measured with an TriStar II Plus apparatus (Micromeritics Instrument Corp). The X-ray absorption find structure spectra (XAFS) (Zn K-edge) were collected at 1W1B station in Beijing Synchrotron Radiation Facility (BSRF). The storage rings of BSRF was operated at 2.5 GeV with an average current of 250 mA. Using Si(111) double-crystal monochromator, the data collection were carried out in transmission/fluorescence mode using ionization chamber. All spectra were collected in ambient conditions.

2.2 Electrochemical measurements

The photocurrent was measured by a conventional three-electrode electrochemical cell with a working electrode, a platinum wire counter electrode and saturated calomel electrode (SCE) as a reference. The working electrode was prepared on Fluorinedoped Tin oxide (FTO) glass, which was cleaned by sonication in acetone, ethanol and deionized water for 30 min each. 5 mg of photocatalyst powder was dispersed in 0.5 mL of dimethylformamide (DMF) under sonication for 2 h to produce slurry. 10 μL of the as-prepared slurry was spread onto the conductive surface of the FTO glass to form a photocatalyst film with an area of 0.25 cm^2. After air drying naturally, the uncoated parts of the electrode were isolated with an epoxy resin. Subsequently, the electrodes were put into an oven at 100 ^oC for 2 h. The working electrodes were immersed in aqueous solution containing 0.1 M Na_2S and 0.1M Na_2SO_3. A 300 W Xenon lamp (PLS-SXE300D, Perfectlight Co., Beijing) with a filter at 400 nm was used as a light source. For Mott-Schottky experiment, the potential ranged from -0.6 to 0.6 V with an increase voltage of 50 mV and the amplitude was 5 mV under the frequency of 500 Hz and 1000 Hz. The measurement was also performed in a conventional three electrode cell, using Pt wire and SCE electrode as the counter electrode and reference electrode, respectively. The electrolyte was 0.2 M Na_2SO_4 aqueous solution without additive (pH = 6.8)

2.3 Photocatalytic test

The photocatalytic reactions were carried out in a photocatalytic hydrogen evolution system (MC-H20II, Merry Change Co., Beijing). 20 mg photocatalyst was suspended in 50 mL of (0.1 M) Na_2SO_3/(0.1 M) Na_2S aqueous solution. 1%Pt was introduced into the reaction system via in-situ photodeposition of H_2PtCl_6. The temperature of the reaction system was 6 ^0C controlled by a circulating thermostatic bath. The suspension was then thoroughly degassed and irradiated with visible light ($\lambda >$ 400 nm) by using a 300 W Xenon lamp (PLS-SXE300D, Perfectlight Co., Beijing). H_2 was detected at set intervals, automatically, by an online gas chromatograph.

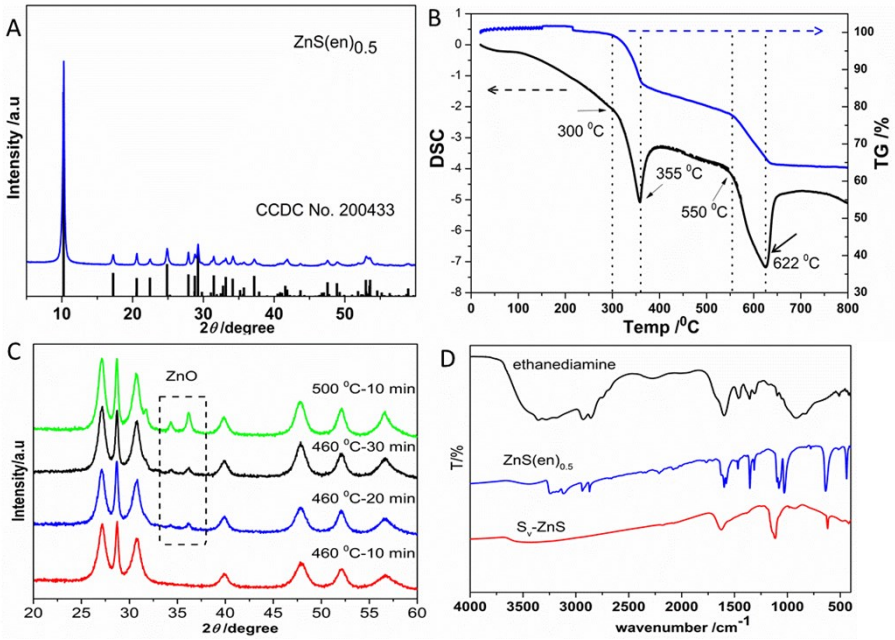

Fig. S1 A) XRD patterns of $ZnS(en)_{0.5}$, B) TG and DSC analysis of $ZnS(en)_{0.5}$, C) XRD patterns of the $ZnS(en)_{0.5}$ calcinated at different temperature and time, D) FTIR spectra of the ethanediamine, $ZnS(en)_{0.5}$ and S_v-ZnS.

Note: As shown the Fig. S1B, the weight loss before 550 ^{0}C and in 550 ^{0}C -620 ^{0}C is about 22.5% and 14.2%, close to the theoretical value of 23.6% ($ZnS(en)_{0.5} \rightarrow ZnS$) and 16.4% ($ZnS \rightarrow ZnO$), respectively.

Note: As shown in Fig. S1C, the XRD patterns demonstrate ZnO is produced when the calcination temperature (T) or time (t) increased. The diffraction peaks at 34.2^0 and 36.2^0 corresponds to the (002) and (101) planes of hexagonal ZnO.

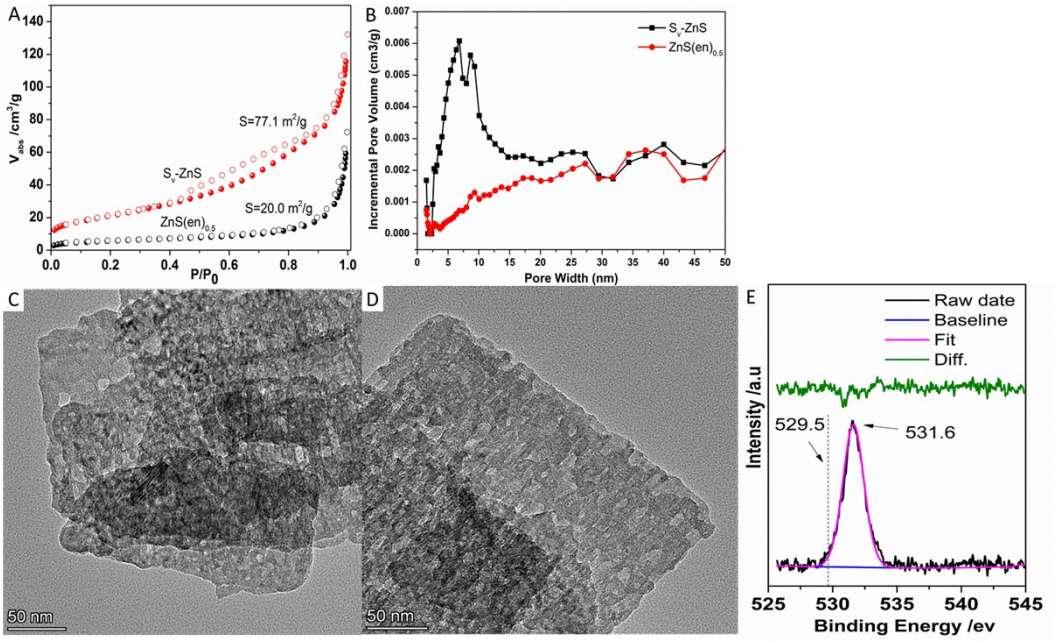

Fig. S2 A) BET absorption at different P/P_0 for $ZnS(en)_{0.5}$ and S_v-ZnS, B) pore size distribution curves of $ZnS(en)_{0.5}$ and S_v-ZnS, C and D) TEM images of S_v-ZnS, E) O 1s xps spectrum of S_v-ZnS.

Note: As shown in Fig. S2E, the O 1s XPS spectrum has a highly symmetric peak centered at 531.6 eV, which is attributed to H_2O or O_2 absorbed on the surface of S_v-ZnS. Generally, O 1s XPS peak of lattice O in metal oxides locates at the binding energy <531.0 eV. It indicates S_v-ZnS does not contain Zn-O bond, further verifying the inexistence of ZnO.

Table 1. EXAFS fitting parameters at the Zn K-edge for various samples

Sample	Shell	N [a]	R (Å) [b]	σ^2 (Å^2·10^{-3}) [c]	ΔE0 (eV) [d]	*R* factor (%)
S_v-ZnS	Zn-S	3.8	2.34	7.4	4.9	0.4
Com-ZnS	Zn-S	**4**	2.35	6.5	5.6	0.3

[a] *N*: coordination numbers; [b] *R*: bond distance; [c] σ^2: Debye-Waller factors; [d] ΔE_0: the inner potential correction. *R* factor: goodness of fit. *S*02 was set as 1.00 for Zn-S , which was obtained from the experimental EXAFS fit of reference ZnS by fixing CN as the known crystallographic value and was fixed to all the samples.

XAFS Analysis and Results. [1-3]

The acquired EXAFS data were processed according to the standard procedures using the ATHENA module implemented in the IFEFFIT software packages. The k3-weighted EXAFS spectra were obtained by subtracting the post-edge background from the overall absorption and then normalizing with respect to the edge-jump step. Subsequently, k3-weighted χ(k) data of Zn K-edge were Fourier transformed to real (R) space using a hanning windows (dk=1.0 Å-1) to separate the EXAFS contributions from different coordination shells. To obtain the quantitative structural parameters around central atoms, least-squares curve parameter fitting was performed using the ARTEMIS module of IFEFFIT software packages.

References:

1. Ravel, B. & Newville, M. ATHENA, ARTEMIS, HEPHAESTUS: data analysis for X-ray absorption spectroscopy using IFEFFIT. *J. Synchrotron Radiat.* **12**, 537-541 (2005).

2. Koningsberger, D. C. & Prins, R. X-ray Absorption: Principles, Applications, Techniques of EXAFS, SEXAFS, and XANES (eds Koningsberger, D. C. & Prins, R.) Vol. 92 (Wiley, 1988).

3. Rehr, J. J. & Albers, R. C. Theoretical approaches to X-ray absorption fine structure. *Rev. Mod. Phys.* **72**, 621-654 (2000).

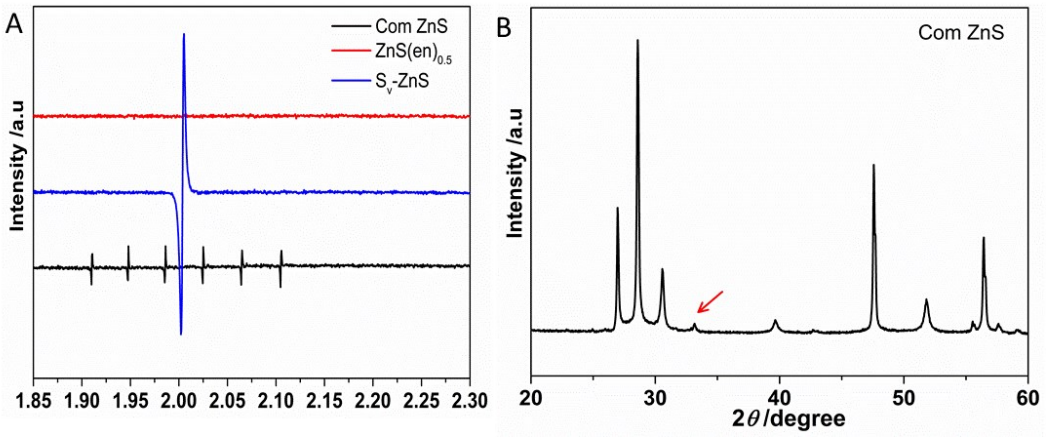

Fig. S3 A) EPR spectra for com ZnS, $ZnS(en)_{0.5}$ and S_v-ZnS; B) XRD patterns of the Com ZnS

Note: As shown in Fig. S3A, the EPR spectrum of com ZnS shows six hyperfine lines with a relatively weak intensity in the range of g=1.9 to g=2.2. The signal is ascribed to the crystal field of cubic ZnS *{ACS Appl. Mater. Interf., 2015, 7, 13915-13924; Chem. Mater., 2004, 16, 915-918; J. Phys-Condens Mat., 2009, 21, 145408}*. The cubic ZnS was the impurity existed in raw hexagonal com ZnS. As shown in Fig. S3B, the very weak peak at 33.3^0 is the diffraction peak of (200) plane of cubic ZnS.

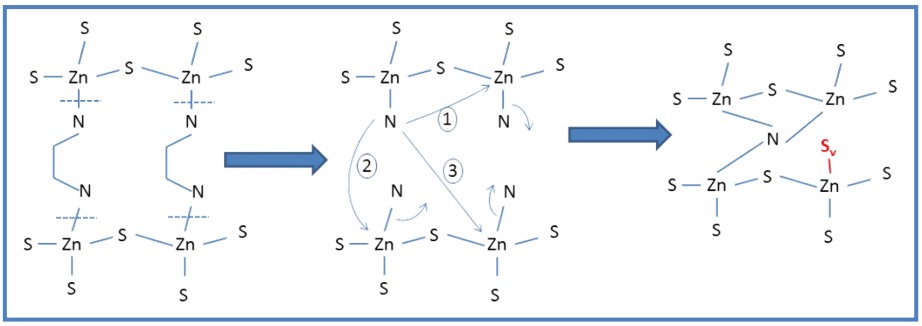

Fig. S4 the proposed process for S_v formation

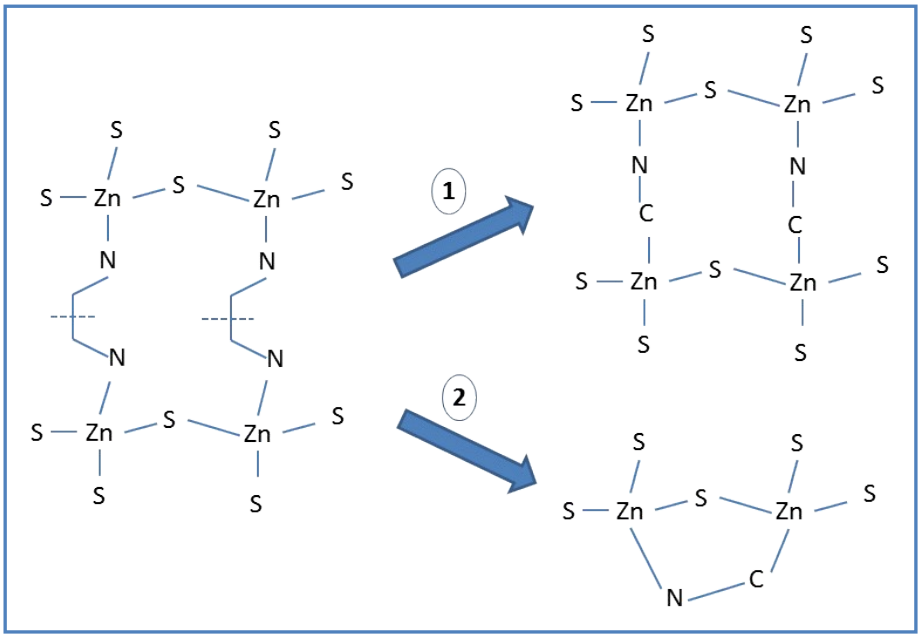

Fig. S5 the proposed process for Zn-C-N-Zn group formation

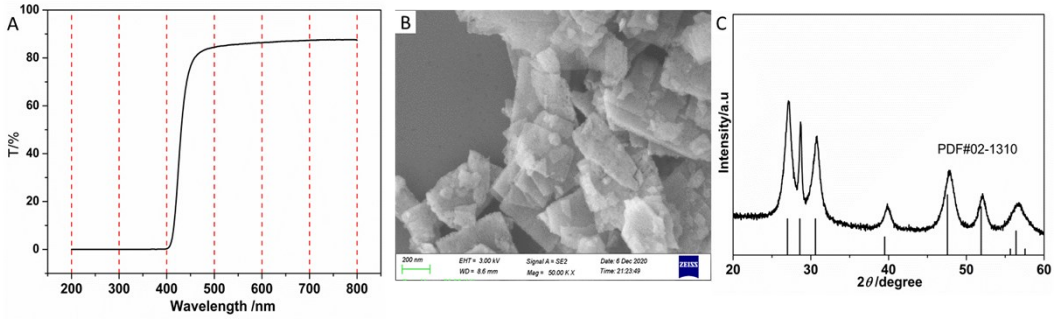

Fig. S6 A) Emission spectrum of the light source via using an optical fitter (λ>400 nm), B) SEM image and C) XRD diffraction patterns of the S_v-ZnS after 6 runs photocatalytic reaction.

Note: As shown in Fig. S6A, only the light (λ>400 nm) can pass through the optical fitter and be used for the exciting light for photocatalysis, indicating that S_v-ZnS is a visible-light photocatalyst.

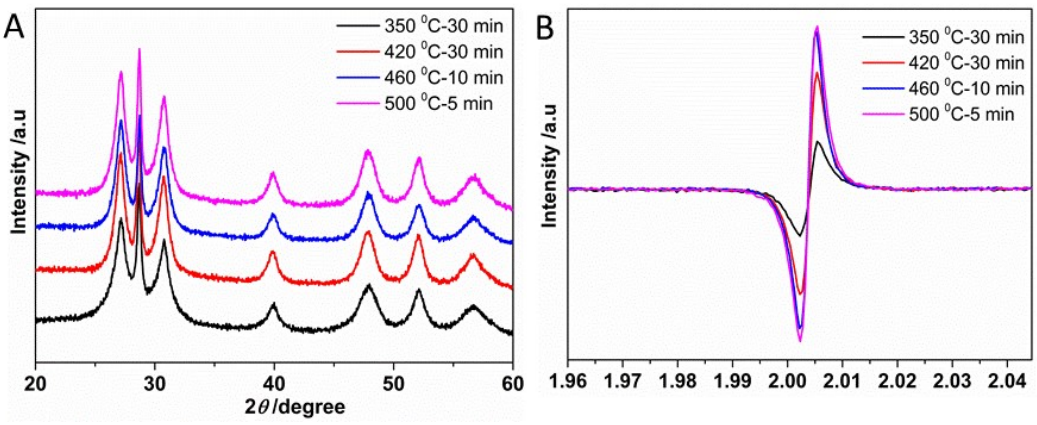

Fig. S7 A) XRD diffraction patterns and B) EPR spectra of S_v-ZnS with various S_v concentrations obtained at different temperature and time.

Note: As shown in Fig. S7A, the obtained samples via calcination at different T and t are all hexagonal ZnS. Additionally, the EPR spectra demonstrate the S_v signals intensities of the samples are different, indicating the concentration of S_v can be adjusted via control of the T and t.

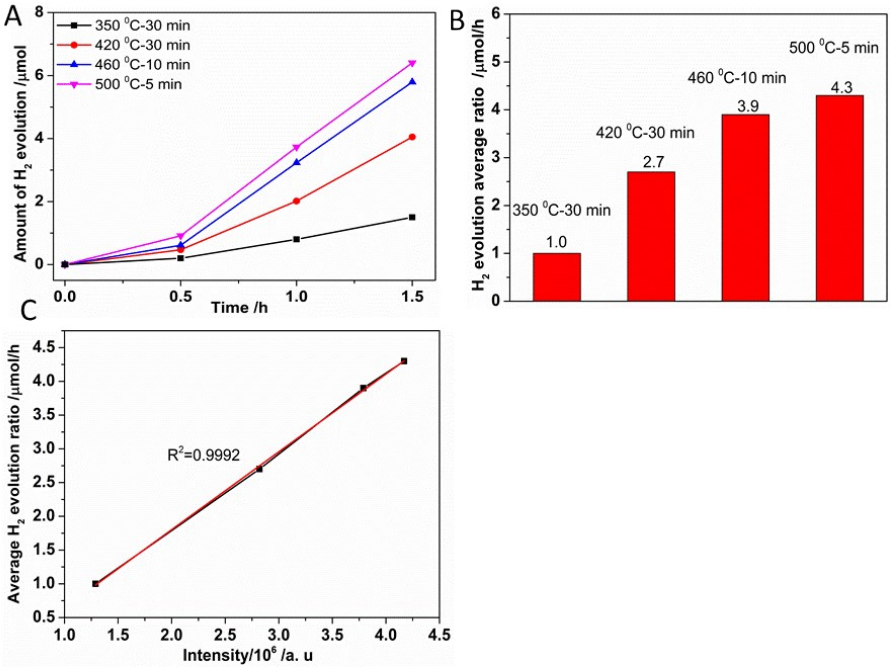

Fig. S8 A-B) time course curves for the photocatalytic H_2 evolution and the corresponding H_2 evolution ratio over the samples with different S_v concentration, C) the relation between S_v signal intensity and H_2 evolution ratio.

Note: As shown, the photocatalytic activities of S_v-ZnS samples shows a positive linear relationship with S_v concentration.